Enhanced Tunnel Magnetoresistance due to Spin Dependent Quantum Well Resonance in Specific Symmetry States of an Ultrathin Ferromagnetic Electrode

Tomohiko Niizeki,[1,*] Nobuki Tezuka,[1,2] and Koichiro Inomata[1,2,3]

[1]*CREST-JST, 4-1-8 Honcho, Kawaguchi, Saitama 332-0012, Japan*

[2]*Department of Materials Science, Tohoku University, Aoba-yama 6-6-02, Sendai 980-8579, Japan*

[3]*National Institute for Materials Science, 1-2-1 Sengen, Tsukuba, Ibaraki 305-0047, Japan*

(Received 28 September 2007; published 31 January 2008)

Spin dependent quantum well resonance has been investigated in fully epitaxial magnetic tunnel junctions with Fe(001)/MgO(001)/ultrathin Fe(001)/Cr(001) structure. The dI/dV spectra clearly show the resonant peaks which shift systematically depending on the thickness of an ultrathin electrode as predicted in *ab initio* calculation [Zhong-Yi Lu *et al.*, Phys. Rev. Lett. **94**, 207210 (2005)]. The magnetotransport is strongly modulated at the same bias voltage as the resonant peaks. This control of the magnetotransport in magnetic tunnel junctions at a specific bias voltage will contribute to the development of active spintronic devices.

DOI: 10.1103/PhysRevLett.100.047207 PACS numbers: 85.75.Mm, 72.25.Ba, 73.21.Fg

Magnetic tunnel junctions (MTJs) have been intensively studied since the discovery of large tunnel magnetoresistance (TMR) at room temperature (RT) [1,2] because of their potential applications in high-density magnetic random access memories and highly sensitive read heads. At first, MTJs with an amorphous AlO_x barrier exhibited TMR ratios of less than 70%. Recently, however, TMR ratios well over 100% have been achieved in MTJs with a crystalline MgO(001) barrier [3–5]. The transport in this structure is called ''coherent tunneling,'' where the electrons conserve the parallel component of their wave vector and propagate according to the symmetry of their wave functions. In a MgO barrier MTJ with body-centered-cubic (bcc) Fe(001) electrodes, for example, *half-metallic* states of Δ_1 symmetry govern the coherent tunneling transport [6,7] and very large TMR has been achieved [3,4].

Coherent tunneling leads to another remarkable quantum mechanical phenomena: spin dependent resonant tunneling (SDRT). The effect is normally considered in double magnetic tunnel junctions which have a very thin middle layer where quantum well (QW) states are created. In the ferromagnetic middle layer, the energy levels of the QW states will be spin split by the exchange interaction. This splitting enables us to select the resonant condition for each spin by applying a certain bias voltage or by changing the electrochemical potential of the middle layer in a three-terminal setup. Since the resonant tunneling via these states is perfectly spin-polarized, one can realize very large TMR at a specific bias voltage.

From an experimental point of view, it is difficult to grow an ultrathin metallic layer on top of the insulating barrier because of the large difference of their surface energy. Recently, Nozaki *et al.* [8] fabricated fully epitaxial Fe/MgO(001) double magnetic tunnel junctions by molecular beam epitaxy and found oscillating component in the differential conductance (dI/dV) spectra possibly due to SDRT. However, the nonuniformity of the Fe QW layer due to island growth on MgO led to a lower peak-to-valley ratio of dI/dV and it was not possible to modulate the dc magnetotransport.

To avoid this island growth, we focus on an alternative structure which incorporates a ''metallic'' layer as a part of the barrier. Considering a fully epitaxial Fe(001)/MgO(001)/ultrathin Fe(001)/Cr(001) structure in the parallel magnetization configuration, we can regard this structure as a double barrier system, where Fe(001) and Cr(001) behave as a half-metal and a ''barrier,'' respectively. This is because only states of Δ_1 symmetry (s character) of Fe(001) and Cr(001) [shown in Figs. 1(a) and 1(b)] can couple efficiently with evanescent sp states in the MgO(001) barrier while the other states, $\Delta_5(pd)$, $\Delta_2(d)$, and $\Delta_{2'}(d)$, rapidly decay [6,7]. Consequently, half-metallic QW states limited to Δ_1 symmetry are created in the ultrathin Fe(001) layer, and the SDRT occurs via these QW states as shown in Fig. 1(c). In the antiparallel magnetization configuration, this structure is no longer a double barrier system except in the case that the potential of Fe/Cr(001) layers is extremely high. States of Δ_1 symmetry cannot contribute to the transport, but the states of other symmetry contribute a little as shown in Fig. 1(d). This large difference between two magnetization configurations will strongly modulate the magnetotransport. Recent *ab initio* calculations by Lu *et al.* [9] predicted staircaselike current-voltage (I-V) curves in the parallel magnetization configuration only and large enhancement of TMR at a specific bias voltage due to this effect.

A similar structure was already investigated by Nagahama *et al.* [10]. They measured magnetotransport of FeCo/AlO_x/ultrathin Fe(001)/Cr(001) MTJs at low temperature, where only Fe(001) and Cr(001) are single crystal. Although they extracted the oscillating component from the dI/dV spectra in the parallel magnetization configuration, it was too subtle an effect to influence the dc magnetotransport. Yuasa *et al.* [11] suggested that the

 © 2008 The American Physical Society

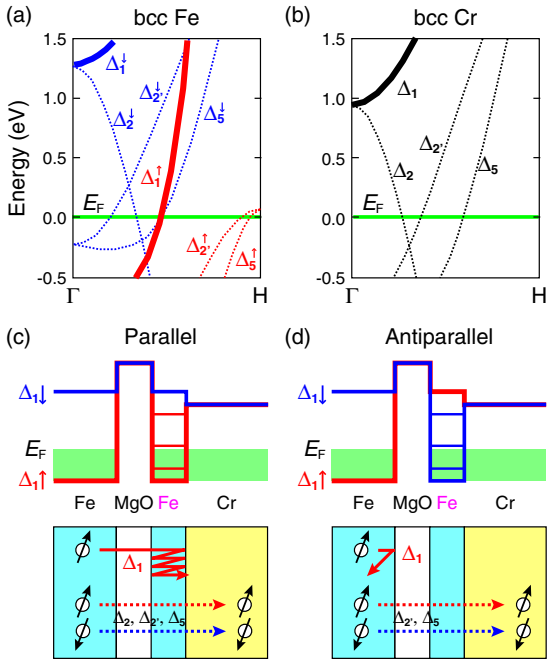

FIG. 1 (color online). (a),(b) Band dispersion of (a) bcc Fe and (b) bcc Cr in the [001] (Γ-H) direction. The red (or gray) [blue (or dark gray)] line in (a) represents majority (minority) spin subbands. The solid and dashed lines represent the states of Δ_1 symmetry and the others, respectively. (c),(d) The potential profiles and schematic illustrations of Fe/MgO/ultrathin Fe/Cr(001) structure in (c) the parallel and (d) the antiparallel magnetization configurations. The red (or gray) and blue (or dark gray) lines represent the potential for spin-up and spin-down states of Δ_1 symmetry, respectively.

subtlety is due to the short mean-free path and spin diffusion length in Fe, but we think it must be mainly due to noncoherent tunneling across an AlO_x barrier.

In order to realize SDRT with a "metallic barrier," a completely coherent system is indispensable. Here, we have investigated the SDRT in fully epitaxial Fe(001)/MgO(001)/ultrathin Fe(001)/Cr(001) MTJs, comparing our data with *ab initio* calculations [9]. We provide clear evidence of the influence of SDRT on dc magnetotransport, and have successfully observed enhanced TMR at a specific bias voltage even at RT.

Top pinned spin-valve–type MTJs with Cr(40)/ultrathin Fe(d)/Mg(0.5)/MgO(2)/Fe(5)/$Co_{75}Fe_{25}$(1)/IrMn(15)/Ta(5) were deposited on single crystal MgO(001) substrates by the combination of sputtering and electron bombardment. Film thickness is in nanometers. The designed thickness of the ultrathin Fe layer (d) was varied from 4 to 10 monolayer (ML) (0.57–1.43 nm). The films were microfabricated into tunnel junctions of (8×8)–(90×90) μm^2 in size by successive microfabrication processes (photolithography, Ar ion milling, SiO_2 sputtering, liftoff, etc.). The dc magnetotransport was measured by the four probe method at 6 K and RT, where bias voltages up to 1.2 V were applied to the MTJs and a magnetic field was applied along the Fe[100] (∥MgO[110]) direction.

We observed TMR ratios of up to 190% at RT, which is comparable to that for the high-quality epitaxial MTJs made by molecular beam epitaxy [4]. The TMR decreases on reducing the ultrathin Fe(001) thickness because of an imperfect antiparallel magnetization configuration (e.g., less than 50% at RT in the case of 5 ML Fe). This imperfect configuration is attributed to the Cr(001) underlayer since bcc Cr(001) is known to have a layered antiferromagnetic structure [12] and the magnetic moments of Fe(001) are antiferromagnetically coupled to the Cr(001) layers at their interface [13]. Moreover, the antiparallel magnetization configuration gets worse at 6 K, where TMR is even less than that for RT in some cases. It is not known if the Néel temperature (T_N) of the Cr(001) underlayer is the same as that for bulk Cr(001) ($T_N = 311$ K) [12], but the magnetization configuration changes drastically just below RT, and then seems to be almost unchanged down to 6 K.

We performed tunnel spectroscopy to investigate the QW effect. Figures 2(a) and 2(b) show the representative dI/dV spectra in the parallel magnetization configuration for $d = 4, 6, 8$ ML and 5, 7, 9 ML, respectively. The dI/dV spectra were obtained numerically from the I-V curves measured at 6 K. We can observe the electronic structure of a bottom (ultrathin) Fe(001) layer at positive bias ($V > 0$) and top Fe(001) layer at negative bias ($V < 0$). The spectra in each graph are very similar, but the two graphs are very different. We can see clear resonant peaks (denoted by black arrows) located at both positive and negative bias in each spectrum. The small dips at zero bias are due to the so-called "zero-bias anomaly," which results from magnon and/or phonon assisted tunneling [14,15]. The sharp peaks at positive bias indicate the creation of discrete energy states in ultrathin Fe(001) [Fig. 2(c)]. These are not normal QW states but are limited to Δ_1 symmetry since the ultrathin Fe(001) is sandwiched by the MgO(001) insulating barrier and the Cr(001) metallic barrier. On the other hand, much smaller peaks and a paraboliclike component can be seen at negative bias. The negative bias transport is governed by resonant tunneling via the QW states below the Fermi level (E_F) [Fig. 2(d)]. The potential height of the tunnel barrier for this resonant tunneling is higher than that for the positive bias transport; thus, the resonant peaks at negative bias become smaller. Once this resonant tunneling participates in the negative bias transport, it acts as a probe for the density of states of the top Fe(001) layer. As a result, the dI/dV spectra have parabolic aspect after the appearance of the resonant peaks.

It is interesting to note that the spectra at positive bias suddenly change to almost linear curves around 1 V. One may think this is just due to the superposition of a nonresonant background component, namely, the contribution of the states of other symmetry such as Δ_2, $\Delta_{2'}$, Δ_5 at E_F which are not negligible in the magnetotransport [16]. However, the interpolation of these curves easily exceeds the spectra at lower bias (i.e., at 0.4 V for $d = 5$ ML), which means these linear curves are not the extension of

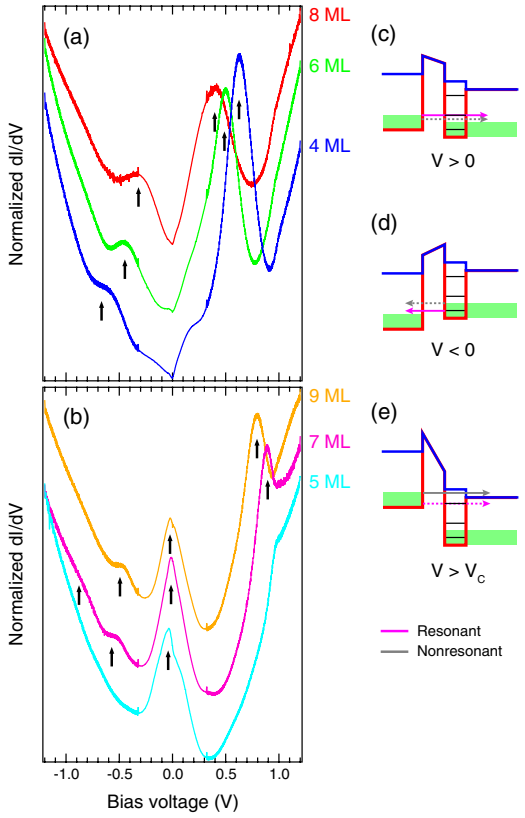

FIG. 2 (color online). (a),(b) The differential conductance (dI/dV) spectra in the parallel magnetization configuration for (a) $d = 4$, 6, 8 ML and (b) 5, 7, 9 ML. Each spectrum is normalized by the minimum value, and is offset. (c)–(e) The potential profiles for the states of Δ_1 symmetry in the parallel magnetization configuration at (c) $V > 0$, (d) $V < 0$, and (e) $V > V_c$. The magenta (or light gray) and gray arrows represent the resonant and nonresonant tunneling, respectively, where the solid line represents dominant transport.

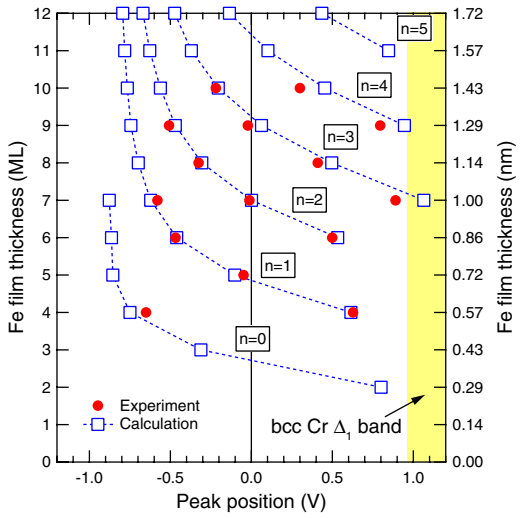

FIG. 3 (color online). Ultrathin Fe(001) layer thickness versus the resonant peak positions. The circles and the squares represent the experimental data and the *ab initio* calculations [9], respectively. The dashed lines categorize the squares by the node number (n) of the standing wave created in the ultrathin Fe(001).

the background component. We must note that the potential height of Cr(001) metallic barrier is about 1 eV, since the bottom edge of the states of Δ_1 symmetry are located around 1 eV in Cr(001) [Fig. 1(c)]. Thus, the spectra have the cutoff voltage V_c above which the resonant tunneling is no longer dominant due to the very short lifetime of the QW states. Instead, the normal tunneling of the states of Δ_1 symmetry govern the transport and give linear curves [Fig. 2(e)].

In order to get the width of the resonant peaks which correlate with the lifetime of the confined electrons, we performed multipeak fitting with Lorentzians. At positive bias, the minimum width of the resonant peak is 0.27 V and the lifetime is estimated to be at least 2.4×10^{-15} sec [17]. The products of this lifetime and the Fermi velocity of Δ_1 state are in good agreement with the majority-spin mean-free path in Fe reported to be about 1 nm [18]. Meanwhile, the width of the peaks near zero bias is difficult to estimate since they are located at slight negative bias and overlap the paraboliclike curves mentioned above.

Finally, the most important data in Fig. 2 remains: namely, the resonant peak positions. Figure 3 shows the ultrathin Fe(001) layer thickness versus the peak positions for our experiment and *ab initio* calculations by Lu *et al.* [9], where the peak positions are defined as the voltages at which the spectra show their local maxima [19]. Lu *et al.* assumed one extra FeO layer on top of the ultrathin Fe(001) layer which they say is inevitable in the deposition process; thus, their indications of the ultrathin Fe(001) layer thickness differ from Fig. 3 by 1 ML. The dashed lines connecting the squares categorize the data by the node number (n) of the standing wave created in ultrathin Fe(001). Our experimental data show remarkably good agreement with the calculations both at positive and at negative bias. The calculations tell us that one resonant state shifts drastically for only a 1 ML change of d. Thus, the great differences in the spectra between Figs. 2(a) and 2(b) are quite normal, while the similarity of the spectra in each graph is superficial. We think the slight difference between our data and the calculations at $n = 3, 4$ is due to the different V_c. Our experiments suggest $V_c \sim 0.95$ V, while V_c seems no less than 1.1 V in their calculation.

Figure 4 shows (a) I-V curves, (b) dI/dV spectra, (c) bias voltage dependence of TMR ratio for $d = 6$ ML measured at both 6 K and RT. In the parallel configuration, the I-V curves are expected to show staircaselike features due to resonant tunneling. We cannot observe such a feature at 6 K, but a bend can be seen around 0.5 V which corresponds to the resonant peak position in the dI/dV spectrum. The corresponding resonant peaks read in the RT dI/dV spectrum, which means the resonant tunneling occurs even at RT. On the other hand, the I-V curves in the antiparallel configuration should have a much more gradual slope at $V < V_c$ than the observed one, since the

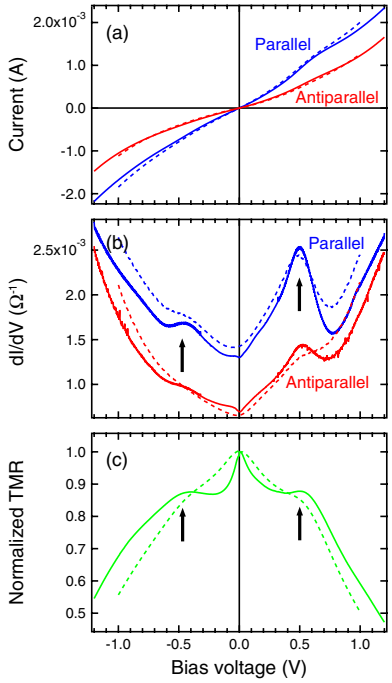

FIG. 4 (color online). (a) I-V curves, (b) dI/dV spectra, (c) bias voltage dependence of TMR ratio for $d = 6$ ML. The blue (or dark gray) [red (or gray)] lines represent the parallel (antiparallel) magnetization configuration. The solid line (dashed line) represents the data measured at 6 K (RT).

states of Δ_1 symmetry do not contribute to the transport. There are two possible causes for the discrepancy: one is the contribution of states of other symmetry and the other is the mixing of the component of the parallel configuration due to the imperfect antiparallel magnetization configuration. Evidence of the latter is clearly seen at the dI/dV spectra between ± 0.5 V, where the spectrum at 6 K exceeds that for RT and shows the peaks at the same position as those in parallel configuration, although the magnitude is much smaller. The bias voltage dependence of the TMR exhibits an encouragingly large $V_{1/2}$ (the voltage at which TMR is halved) and clear enhancement at a bias voltage corresponding to the resonant peaks even at RT. By changing the bottom Fe layer thickness, we can easily tune the voltage at which TMR is enhanced. Further reduction of the background component in dI/dV and realization of better antiparallel magnetization alignment are required in order to approach the ideal staircase behavior of I-V and further enhanced TMR.

In conclusion, dI/dV spectra in the fully epitaxial Cr/ultrathin Fe/MgO/Fe(001) MTJs show clear evidence of the QW resonant states limited to Δ_1 symmetry. The TMR is clearly enhanced at the bias voltage corresponding to the resonant peaks even at RT. This is the first observation of the QW confinement by a metallic barrier for the states of specific symmetry. Additionally, it provides direct evidence of the Δ_1 symmetry-sensitive tunneling across a crystalline MgO(001) barrier, which had not been proved experimentally. The spin dependent QW resonance provides a powerful means to control the dc magnetotransport of MTJs at a specific bias voltage and can therefore be expected to contribute to the development of new generation spintronic devices which integrate a memory cell of magnetic random access memory with a selecting diode.

The authors are grateful to J. M. D. Coey for reviewing the manuscript and to T. Nozaki, Y. Sakuraba, and X.-G. Zhang for helpful discussions. Part of this study was performed with equipment of Miyazaki Laboratory in Tohoku University.

*niizekit@tcd.ie

[1] T. Miyazaki and N. Tezuka, J. Magn. Magn. Mater. **139**, L231 (1995).
[2] J. S. Moodera, L. R. Kinder, T. M. Wong, and R. Meservey, Phys. Rev. Lett. **74**, 3273 (1995).
[3] S. S. P. Parkin, C. Kaiser, A. Panchula, P. M. Rice, B. Hughes, M. Samant, and S.-H. Yang, Nat. Mater. **3**, 862 (2004).
[4] S. Yuasa, T. Nagahama, A. Fukushima, Y. Suzuki, and K. Ando, Nat. Mater. **3**, 868 (2004).
[5] D. D. Djayaprawira, K. Tsunekawa, M. Nagai, H. Maehara, S. Yamagata, N. Watanabe, S. Yuasa, Y. Suzuki, and K. Ando, Appl. Phys. Lett. **86**, 092502 (2005).
[6] W. H. Butler, X.-G. Zhang, T. C. Schulthess, and J. M. MacLaren, Phys. Rev. B **63**, 054416 (2001).
[7] J. Mathon and A. Umerski, Phys. Rev. B **63**, 220403(R) (2001).
[8] T. Nozaki, N. Tezuka, and K. Inomata, Phys. Rev. Lett. **96**, 027208 (2006).
[9] Zhong-Yi Lu, X.-G. Zhang, and S. T. Pantelides, Phys. Rev. Lett. **94**, 207210 (2005).
[10] T. Nagahama, S. Yuasa, Y. Suzuki, and E. Tamura, J. Appl. Phys. **91**, 7035 (2002).
[11] S. Yuasa, T. Nagahama, and Y. Suzuki, Science **297**, 234 (2002).
[12] J. Unguris, R. J. Celotta, and D. T. Pierce, Phys. Rev. Lett. **69**, 1125 (1992).
[13] R. Jungblut, Ch. Roth, F. U. Hillebrecht, and E. Kisker, J. Appl. Phys. **70**, 5923 (1991).
[14] S. Zhang, P. M. Levy, A. C. Marley, and S. S. P. Parkin, Phys. Rev. Lett. **79**, 3744 (1997).
[15] J. S. Moodera, J. Nowak, and R. J. M. van de Veerdonk, Phys. Rev. Lett. **80**, 2941 (1998).
[16] C. Tiusan, M. Sicot, J. Faure-Vincent, M. Hehn, C. Bellouard, F. Montaigne, S. Andrieu, and A. Schuhl, J. Phys. Condens. Matter **18**, 941 (2006).
[17] We cannot exclude the possibility of inhomogeneous broadening due to well width fluctuation. Thus, this value is thought to be the lowest possible estimate.
[18] A. Enders, T. L. Monchesky, K. Myrtle, R. Urban, B. Heinrich, J. Kirschner, X.-G. Zhang, and W. H. Butler, J. Appl. Phys. **89**, 7110 (2001).
[19] In the case of the broad peaks showing no local maximum such as peaks for negative bias, we used the second derivative of I-V curves to determine it.